Osteoarthritis Cartilage. Author manuscript; available in PMC 2016 November 10.

Published in final edited form as:

Osteoarthritis Cartilage. 2009 November ; 17(11): 1453–1460. doi:10.1016/j.joca.2009.05.004.

Quantitative analysis of subchondral sclerosis of the tibia by bone texture parameters in knee radiographs: site-specific relationships with joint space width

A. K. O. Wong[†,*], **K. A. Beattie**[‡], **P. D. Emond**[§], **D. Inglis**[||], **J. Duryea**[¶], **A. Doan**[§], **G. Ioannidis**[§], **C. E. Webber**[#], **J. O'Neill**[††], **J. de Beer**[††], **J. D. Adachi**[††], and **A. Papaioannou**[§]

[†]Department of Medical Sciences, McMaster University, Hamilton, ON, Canada

[‡]Department of Medicine, McMaster University, Hamilton, ON, Canada

[§]Department of Medical Physics, McMaster University, Hamilton, ON, Canada

[||]Department of Civil Engineering, McMaster University, Hamilton, ON, Canada

[¶]Department of Radiology, Brigham and Women's Hospital, Harvard Medical School, Boston, MA, USA

[#]Department of Nuclear Medicine, Hamilton Health Sciences, McMaster University, Hamilton, ON, Canada

[††]Department of Medicine, McMaster University, St. Joseph's Healthcare, Hamilton, ON, Canada

Summary

Objectives—To determine the ability of radiographic bone texture (BTX) parameters to quantify subchondral tibia sclerosis and to examine clinical relevance for assessing osteoarthritis (OA) progression. We examined the relationship between BTX parameters and each of (1) location-specific joint space width (JSW) [JSW(x)] and minimum JSW (mJSW) of the affected compartment, and (2) knee alignment (KA) angle in knee radiographs of participants undergoing total knee arthroplasty (TKA).

Design—Digitized fixed-flexion knee radiographs were analyzed for run-length and topological BTX parameters in a subchondral region using an algorithm. Medial JSW(x) was computed at x = 0.200, 0.225, 0.250 and 0.275 according to a coordinate system defined by anatomic landmarks. mJSW was determined for medial and lateral compartment lesions. KA angles were determined from radiographs using an anatomic landmark-guided algorithm. JSW measures and the magnitude of knee malalignment were each correlated with BTX parameters. Reproducibility of BTX parameters was measured by root-mean square coefficients of variation (RMSCV%).

Results—Run-length BTX parameters were highly reproducible (RMSCV% < 1%) while topological parameters showed poorer reproducibility (>5%). In TKA participants (17 women, 13

[*]Address correspondence and reprint requests to: A. K. O. Wong, Department of Medical Sciences, McMaster University, 501-25 Charlton Ave E, Hamilton, ON L8N 1Y2, Canada. Tel: 1-905-527-9100; Fax: 1-905-521-1297; wongko@mcmaster.ca.

Conflict of interest

Disclosure statement: none of the authors have relevant conflicts of interest to declare.

men; age: 66 ± 9 years; body mass index (BMI): 31 ± 6 kg m^{-2}; WOMAC: 41.5 ± 16.1; Kellgren–Lawrence score mode: 4), reduced trabecular spacing (Tb.Sp) and increased free ends (FE) were correlated with decreased JSW after accounting for BMI, gender and knee malalignment. These relationships were dependent on site of JSW measurement.

Conclusion—High reproducibility in quantifying bone sclerosis using Tb.Sp and its significant relationship with JSW demonstrated potential for assessing OA progression. Increased trabecular FE and reduced porosity observed with smaller JSW suggest collapsing subchondral bone or trabecular plate perforation in advanced knee OA.

Keywords

Severe osteoarthritis; Bone texture parameters; Radiograph; Subchondral bone; Location-specific joint space width

Introduction

Abnormal loading in the medial and lateral tibial compartments is thought to be a risk factor for progressive knee osteoarthritis (OA)[1]. As a result of altered biomechanics, cartilage thinning ensues and has been characterized as a hallmark of OA progression. As a surrogate measure of cartilage thickness, decreased joint space width (JSW) is representative of reduced cartilage thickness and therefore a worsened OA disease state[2,3]. More recently, Duryea *et al.* described the use of a location-specific JSW [JSW(*x*)] algorithm which demonstrated higher reproducibility[2] and sensitivity to OA changes[4], particularly at a site 22.5% internal to the tibial borders, compared to both minimum JSW (mJSW) and Kellgren–Lawrence (KL) scores. When joint space is narrowed in one compartment, the knee becomes malaligned and further contributes to unequal load distribution and exacerbated damage to one compartment. Knee malalignment has been shown to be a significant predictor of OA progression in both medial and lateral compartments[5], particularly in patients with moderate OA[6]. Although cartilage degeneration has been identified as the idiosyncratic feature of OA, there is interest in the subchondral bone that accompanies altered mechanical loading.

Alterations in subchondral bone structure may be reflected by increased subchondral sclerosis. Subchondral sclerosis, as identified by regions of high attenuation in knee radiographs, is purported to result from increased bone mineral density (BMD) and bone volume fraction (BVTV) in OA[7]. These high attenuation regions located adjacent to the cortical bone–cartilage interface at the site of degeneration are notable in early stages of disease, and arguably occur before apparent joint space narrowing[8]. Increased vascularity and subchondral bone turnover have been revealed in the pathogenesis of joint destruction[9,10]; though whether bone remodelling in the subchondral region of affected compartments is concomitant to initial cartilage degeneration or precedes it remains unknown[11]. Radin *et al.* were one of the first to postulate the influence of subchondral plate thickening on cartilage stress[12–15]. It is thought that reduced load distribution throughout the subchondral trabeculae results in greater strains on the articular cartilage, thus subjecting it to increased frictional damage[16]. In fact, the condition of articular cartilage depends on mechanical properties of subchondral bone such as density and trabecular architecture[16].

Currently, there is a lack of knowledge regarding structural changes that occur in the subchondral trabeculae in progressive knee OA with altered mechanical loading. Hence, there is motivation to investigate progressive changes in the subchondral bone to determine whether there is an influence on cartilage degeneration. While high resolution peripheral quantitative computed tomography can non-invasively provide bone architecture information, it is challenged by beam hardening artifacts at thick cortical bone, a high radiation dose, and difficulty accessing peripheral sites as the knee. Therefore, we assessed bone sclerosis on film radiographs achievable through the widely available X-ray modality.

To date, subchondral sclerosis has only been assessed as a dichotomous outcome using the Altman radiographic atlas by identifying its presence (1) or absence (0)[17]. In fact, it may be difficult to visually discern whether or not sclerosis is present. Several studies measured the degree of anisotropy of subchondral sclerosis by analyzing digitized film radiographs in 2D[18–23]. Pothaud *et al.* demonstrated that fractal dimension coupled with BMD can predict trabecular connectivity[23]. More recently, fractal signature analysis provided fractal dimension for vertical and horizontal trabeculae independently at different widths[24].

Few studies have directly investigated topological and run-length parameters from plain radiographs. Such 2D assessments can be extrapolated to 3D through binary image analysis[24–26]. Topological parameters describe object orientation and connectedness including apparent trabecular free ends (FE), network length (NL), nodal points (Nd) and an overall connectivity index (CI). Run-length parameters describe metric properties between objects such as apparent trabecular number (Tb.N), trabecular spacing (Tb.Sp), trabecular thickness (Tb.Th) and BVTV. Together, these parameters can be used to quantify bone texture (BTX) in regions of subchondral sclerosis. The degree of subchondral sclerosis may give clues as to the underlying changes in subchondral bone architecture and hence changes in load distribution in the bone that purportedly contribute to cartilage degeneration. As a first step to determine changes in subchondral bone with OA, the current cross-sectional study will test the hypothesis that more sclerotic subchondral bone as quantified using topological and run-length BTX parameters is related to more severe joint space narrowing and greater knee malalignment. We anticipate that BTX parameters are candidates for clinically relevant and reproducible outcome measures in OA.

Method

PARTICIPANTS

Participants were selected from a study analyzing articular cartilage morphometry in a pre-arthroplasty OA population. This group included participants who were candidates for total knee arthroplasty (TKA) as a result of single or bilateral knee OA, as defined by the American College of Rheumatology criteria, and were recruited through an orthopaedic surgeon (JDB) at Hamilton Health Sciences (Henderson Campus, Hamilton, ON, Canada). TKA was indicated in these participants as a result of failure on non-surgical management and patients' well-informed risk–benefit assessment for surgery. All participants had previously consented to undergo X-rays of their affected knee(s) and to complete the Western Ontario McMaster Universities OA index (WOMAC) survey. This study was

approved by the Research Ethics Board at McMaster University and Hamilton Health Sciences.

RADIOGRAPHY

Posteroanterior (PA) radiographs acquired using the fixed-flexion technique[27] were obtained from each OA-affected knee. Film radiographs from X-ray were digitized using a VIDAR® Sierra Plus digitizer (Herndon, VA) configured at a bit depth of 12 and 300 dpi resolutions. Investigators performing radiographic assessments and analyses were blinded to the health status and demographics of the participants. KL score for each knee radiograph was assessed by a single radiologist (JO).

BTX ANALYSIS ALGORITHM

Digitized knee radiographs were analyzed for BTX parameters (Table I) using a semi-automated algorithm. Subchondral regions of interest (ROIs) in the tibia were situated using a locator rule in which endpoints were placed on the outer cortical edges of the medial and lateral non-osteophytic tibial borders immediately inferior to the cortical bone–cartilage interface (Fig. 1). These landmarks defined the overall width of the tibial plateau (Tw). The locator rule automatically constructed circular ROIs such that their diameters equalled 0.20 × Tw and were positioned distal to the locator rule (in proximity to the bone–cartilage interface) at a distance equal to 0.15 × Tw and with edges of the ROI internal to the ends of the locator rule at a 0.065 × Tw distance.

From the ROIs constructed in the medial and lateral subchondral compartments, BTX parameters for both ROIs were calculated automatically using equations shown in Table I, which were based on binary and skeletonized images converted from digitized radiographs by threshold pixel values separating bone (1) from marrow space (0)[28]. The calculation of run-length parameters employed the run-length method as described by Parfitt and Durand[29,30]. It is noteworthy that BTX parameters provide only apparent structural information. Hence, our reference to structural information does not imply true 3D architecture. Analyses for BTX parameters were performed only for ROIs on the affected side(s) as evidenced by apparent joint space narrowing. BTX parameters were measured in triplicate on three separate days by a single user (AKOW).

MINIMUM AND LOCATION-SPECIFIC JSW

Analyses for JSW(x) were performed using a semi-automated software tool which delineated femoral and tibial compartment contours [Fig. 2(a)][2]. A coordinate system was constructed with an x-axis represented by a line tangent to both femoral epicondyles. A y-axis and an $x = 1.0$ line were positioned perpendicular to the x-axis and tangent to the medial and lateral femoral contour edges [Fig. 2(a)]. JSW measures were determined at the $x = 0.200$, 0.225, 0.250 and 0.275 sites using the described coordinate system for the affected medial compartment only [Fig. 2(b)]. Minimum JSW was computed for both medial and lateral compartments. All JSW(x) analyses were performed by one reader (JD) and mJSW analyses performed by another reader (KAB).

KNEE ALIGNMENT (KA) MEASUREMENT

KA was measured using a computer algorithm previously described[31]. The resultant anatomic angle (θ_A) subtended by the constructed axes was converted to a mechanical angle (θ_M) according to an equation determined by Kraus and colleagues[32]:

$$\theta_M = (0.69 \times \theta_A) + 53.69 \quad (1)$$

mechanical KA was expressed as degrees of deformity from a quoted 'normal' KA of 178.5° by Moreland *et al.*[33]. Because both varus and valgus deformities were identified among participant knees, the absolute value of KA deformity was employed [magnitude of KA deformity (mKAD)] for correlation analyses with BTX parameters. Alternatively, the relative KA deformities (rKAD) expressed as positive and negative from normal were used as covariates. All KA measures employed in the current study were means of measurements obtained by two readers (KAB and AKOW) on two occasions ($n = 4$) (Fig. 3).

DATA ANALYSES

BTX parameters were expressed as means [±2 standard deviations (SD)] ($n = 3$). For all analyses, topological BTX parameters were divided by ROI area to account for inter-participant variation in ROI size. Intra-rater reproducibility was assessed using root-mean square coefficients of variation (RMSCV%) for the first two repetitions performed on separate days. Medial JSW(x), medial and lateral mJSW, and mKAD were each correlated with all BTX parameters using a simultaneous multivariate regression analysis while accounting for age, gender and body mass index (BMI) covariates as independent variables. For JSW(x) correlations, mKAD and rKAD were also included in covariate analysis. Unstandardized partial regression coefficients (B) ±2 SD were reported.

Results

REPRODUCIBILITY OF BTX MEASUREMENTS

In our sample of 30 TKA participants (see Table II for participant characteristics), BTX measurements demonstrated modest reproducibility (Table III). Precision errors were close to 1% for all run-length parameters. However, for topological parameters, such as Nd and CI, measurement error approached or exceeded 10%. There was particularly poorer agreement between repeat CI measurements despite acceptable reproducibility of FE and NL parameters, which were used to compute CI. All mean measures of BTX parameters (±2 SD) derived from the subchondral ROI of the affected tibial compartment are reported in Table IV.

RELATIONSHIP BETWEEN MEDIAL JSW(x) AND BTX PARAMETERS

Tables V and VI illustrate the overall correlations observed between medial JSW(x) and BTX parameters. With smaller Tb.Sp, JSW(x) appeared to decrease at all four sites as demonstrated by positive regression coefficients, thus supporting our hypothesis that greater sclerosis is associated with greater joint space narrowing. However, this relationship was only significant at the $x = 0.200$ site after accounting for gender and BMI. Notably,

correlation coefficients for Tb.Sp vs JSW(x) increased in value from $x = 0.275$ towards the more medial location ($x = 0.200$). As a second characteristic of increased sclerosis, a higher number of trabecular FE was correlated with smaller JSW at all sites, which was again significant after adjusting for differences in BMI, but only at the more lateral JSW(x) sites: $x = 0.250$ and $x = 0.275$. Interestingly, when we accounted for mKAD, a stronger correlation was observed.

While we hypothesized that an increase in sclerosis on radiographs can also be represented by a greater BVTV, Tb.Th, Nd, NL and overall increase in CI, we did not observe a significant correlation between any of these parameters and lower JSW(x) values. A greater Nd and CI did tend towards lower JSW(x), but the relationship was not significant.

RELATIONSHIP BETWEEN MEDIAL AND LATERAL MJSW AND BTX PARAMETERS

Although we were only able to measure JSW(x) for the medial compartment in our participants, we discovered very similar correlations between BTX parameters and mJSW at both medial and lateral compartments as we had for medial JSW(x). Table VII illustrates these relationships. An increase in sclerosis as represented by a higher number of trabecular FE, Nd and decreased Tb.Sp were correlated with a lower mJSW, again supporting the notion that greater subchondral sclerosis is related to joint space narrowing. Notably, all mJSW correlations were greater than correlations obtained at all four sites but were closer to the JSW($x = 0.200$) site. Using mKAD to account for varus and valgus alignment appeared to play an important role in these analyses.

mKAD AND BTX PARAMETERS

No apparent correlations were identified between mKAD and each BTX parameter even after adjustment for age, gender and BMI covariates (data not shown).

Discussion

Our study quantified subchondral bone sclerosis from knee radiographs in an OA cohort with advanced disease requiring TKA. The analysis of BTX parameters performed using our custom designed software algorithm showed short-term reproducibility, at least for intra-observer measurements. We identified modest relationships between more sclerotic bone, as represented by decreased porosity and an increased number of trabecular FE, and two measures of JSW. In each case, one or more covariates, namely BMI, age, gender and KA deformity contributed to the variability in BTX parameter measures. These relationships may depend on the site at which JSW is measured. On the other hand, the mKAD did not correlate with BTX parameters.

BTX ALGORITHM REPRODUCIBILITY

Our previous reproducibility study on digital KA assessment suggested that consistent anatomic landmark selection reduced measurement error[31]. Here, we have once again demonstrated reasonable reproducibility for BTX parameter measurements by using a fixed set of anatomic landmarks to locate ROIs. These data represent the first attempt at determining short-term reproducibility for individual BTX parameter measurements in

digitized radiographs. Previous data on subchondral bone measurement reproducibility have been published for analyses on fractal dimension[23]. A potential source of variability in our study is the presence of osteophytes rendering tibial border identification difficult and resulting in variation in ROI placement. It is possible that the poorer reproducibility of topological parameters resulted from the wider variability in skeletonized structures due to the projectional nature of 2D radiographs; namely that the 2D image is a rendition of a series of stacked trabeculae. One should, however, be cautious as to the interpretation of BTX parameters; while they may serve as good candidates for quantifying bone sclerosis and provide an indication of bone health status, they may not necessarily represent true architecture of trabecular bone throughout a volume of interest.

REDUCED POROSITY AND INCREASED TRABECULAR FE IN ADVANCED KNEE OA

Our data suggest that in more advanced stages of OA with JSW narrowing, porosity is reduced and subchondral trabeculae exhibit more FE in the affected compartment. This observation demonstrates that BTX parameters are quantitative measures representing sclerosis that are clinically relevant. A possible explanation for this phenomenon is subchondral bone collapse under sustained loading conditions. This event is not surprising since subchondral bone turnover is increased in knee OA[9–11,34] while bone quality is compromised due to lack of proper mineralization[35]. In fact, one recent study indicated that volumetric BMD in the posterior subchondral region is low despite the sclerosis observed[36]. Although Bruyere *et al.* provided clinical evidence that increased subchondral BMD was a predictor for lower JSW, they measured areal BMD using dual-energy X-ray absorptiometry[37], which may be the result of compressed trabeculae combined to give an apparently higher BMD. Following our hypothesis, subchondral bone collapse would lead to a lack of trabecular bone network to redistribute biomechanical loads. Hence, joint space narrowing may result from the thickened subchondral bone as previously purported[12,38].

That we reported higher trabecular FE in participants with smaller JSW values further supports the notion that trabeculae may have collapsed in the subchondral region. A high number of FE is suggestive of poor connectivity, particularly that resulting from perforation of trabecular struts. However, subchondral bone collapse and resultant microfractures in the trabeculae may be responsible for the observed FE increase, especially as bone volume did not appear to be compromised. While we observed higher connectivity in participants with lower JSW, the relationship was not significant and may be a consequence of measuring BTX from a projectional image. Although our BTX parameters may not truly represent volumetric bone structure, higher resolution imaging may help determine the source of increased FE.

Other investigators have found that in late-stage OA, osteoporosis occurs in the subchondral bone of the tibia subsequent to subchondral bone sclerosis[35,39–42]. Osteoporosis can occur due to abnormal loading in the tibial compartments when subchondral bone is dense and load distribution is reduced. In some instances, the resultant osteoporotic subchondral bone can result in late-stage OA tibial compartment collapse[35,40]. Weakness in trabecular bone certainly explains the possibility that the subchondral compartment can collapse and result in reduced Tb.Sp and an increase in the number of FE. So far, our hypotheses for a

collapsing subchondral compartment were based on an advanced-stage disease cohort. However, the initial subchondral plate thickening preceding compromised bone quality and subchondral collapse may, in fact, be observed in earlier stages of OA. Such bone thickening in the subchondral compartment may be the result of endochondral ossification[43–46].

Various factors such as postmenopausal status, vitamin D intake and level of weight-bearing activity may control whether altered load distribution in the proximal tibia necessarily proceeds to osteoporotic changes in the subchondral bone. In the Chingford study, Bettica and colleagues demonstrated that women with stable knee OA tend not to exhibit increased bone resorption compared to those with progressive knee OA[47]. This study was more recently corroborated by a 2-year longitudinal study of progressors and non-progressors of OA. In fact, it has been suggested that the groups with progressive knee OA exhibited higher subchondral bone turnover than those with stable OA[35]. These observations suggest that two groups of patients may exist, each of whom respond to altered load distribution in the proximal tibia differently. While it is most probable that our TKA participants had progressive knee OA, there may be multiple factors influencing this dichotomy. Consequently, longitudinal assessment of BTX parameters in OA populations may become difficult. Prospective studies designed to determine whether BTX parameters may be predictors of whether OA patients are progressors or non-progressors of disease would be an important next goal.

LACK OF CORRELATIONS BETWEEN mKAD AND BTX PARAMETERS

It was surprising to discover that KA did not correlate with any of the BTX parameters even after covariate analysis, particularly since it is intimately related to JSW. Linear regression analysis for JSW vs KA revealed B coefficients at −0.63 ($P = 0.074$), and −0.57 ($P < 0.001$) for mJSW and JSW($x = 0.275$), respectively. The relationship between JSW and KA only explained about 30% of the variance ($r^2 = 0.298$–0.310) in the two variables; part of the unexplained variance may describe why KA correlated so poorly with BTX parameters. Certain patients with negligible knee malalignment may have both medial and lateral compartment lesions. The subset of patients exhibiting dual compartment compression may consequently offset the correlations between KA and BTX parameters.

DIFFERENCES IN JSW(x) SITES

Although high short-term reproducibility of JSW(x) measurements was shown for the medial compartment of OA and healthy participants, the reproducibility of those with lateral compartment disease is unknown[4]. In fact, delineating the lateral tibial plateau and femoral condyles during JSW measurement was difficult for patients with lateral compartment lesions, especially since the PA fixed-flexion view is sub-optimal for viewing the lateral compartment[2]. The algorithm for defining lateral compartment JSW(x) has yet to be refined. However, we have reported mJSW relationships for the lateral compartment and showed similar relationships with BTX parameters when analyses were focused only on the medial compartment for JSW(x). While we saw a general increase in JSW(x) values from the $x = 0.200$ to $x = 0.275$ locations, the increase was not significant. Meanwhile, we did notice that BTX parameter correlations with JSW(x) were site-specific. We speculate that differences in porosity would most likely be reflected in more medial regions where mechanical loading is

greater, and perhaps more apparent with influence of greater knee malalignment. On the other hand, trabecular FE purportedly resulting from trabecular plate perforation may be more susceptible towards the lateral region where mechanical loading is lost.

LIMITATIONS AND FURTHER RESEARCH

We acknowledge that there are several limitations to our study. Given the fact our sample of 30 participants was restricted to patients requiring TKA, only those with more advanced disease were included thus challenging the generalizability of our results to those with mild or moderate OA. In fact, the range of JSW values for our TKA participants was relatively narrow. It is possible that a cohort encompassing a larger range of participants with varying disease severity would provide stronger and more resolved relationships between JSW and BTX parameters.

The technology of plain X-ray imaging limits the ability to accurately determine BTX parameters that are fully representative of 3D subchondral bone architecture in the tibia. Hence, there are certainly regions of the subchondral bone in 3D space that cannot be captured by 2D radiographs. Overlapping trabeculae may appear as apparent connectivity, in effect skewing the computed topological parameters. It is possible, however, that these parameters may be useful in the longitudinal measurement of OA progression, although this has yet to be examined. In order to determine whether these BTX parameters show construct validity against true bone architecture, we will require comparison with bone structure from microcomputed tomography.

We investigated a subchondral region of the tibia more distal from the cortical plate than defined in other studies[35,48,49]. Buckland-Wright *et al.* investigated a rectangular ROI 100 pixels in height, positioned at the internal three quarters of the tibial compartment immediately inferior to the cortical plate[35]. Whereas changes just beneath the cortical plate may be more physiologically connected to articular cartilage integrity[50], Li and Aspden formerly suggested that cancellous bone changes in OA may not only be localized to the joint surface, but can be generalized throughout cancellous bone of the joint[51]. Our more distal subchondral region exhibited similar trends in BTX parameters with OA progression identified by investigators who examined subchondral bone immediately inferior to the cortical plate[35,52]. Brown *et al.* scanned juxtaarticular, epiphyseal and metaphyseal regions of the proximal tibia to characterize subchondral bone defects in inner and outer sections[48]. Future studies investigating BTX parameters in these separate regions may prove useful in characterizing regional differences in bone sclerosis.

Conclusions

In the subchondral bone of the tibia, greater joint space narrowing appears to be associated with lower porosity and a greater number of free trabecular ends. Covariates (BMI, gender, age and KA angle) significantly contributed to these relationships. Meanwhile, KA angle did not correlate with BTX parameters since it did not account for patients with dual compartment narrowing. The use of BTX parameters as predictors of rapid OA progression may guide future diagnosis and treatment. The next step is to perform a longitudinal study to determine the predictive value of BTX parameters on rapid OA progression. Based on the

pattern of bone distribution observed, we hypothesize that patients with advanced knee OA exhibit subchondral bone collapse. Despite the cross-sectional nature of our study and the sole inclusion of TKA participants, it is a first step in elucidating BTX properties in progressive knee OA through digitized knee radiographs. In addition, the ease of use and reasonable reproducibility of these parameters will improve feasibility in future clinical studies.

Acknowledgments

We would like to thank our funding from the CIHR Strategic Training Program in Skeletal Health Research (STP 53892).

Abbreviations

OA	osteoarthritis
TKA	total knee arthroplasty
BVTV	bone volume fraction
CI	connectivity index
Nd	number of nodes
NL	network length
FE	number of free trabecular ends
Tb.Sp	trabecular spacing
Tb.Th	trabecular thickness
JSW(*x*)	location-specific joint space width
mKAD	magnitude of knee alignment deformity
rKAD	relative knee alignment deformity

References

1. Hsu RW, Himeno S, Coventry MB, Chao EY. Normal axial alignment of the lower extremity and load-bearing distribution at the knee. Clin Orthop Relat Res. 1990 Jun.(255):215–27.
2. Duryea J, Zaim S, Genant HK. New radiographic-based surrogate outcome measures for osteoarthritis of the knee. Osteoarthritis Cartilage. 2003 Feb; 11(2):102–10. [PubMed: 12554126]
3. Buckland-Wright JC, Macfarlane DG, Williams SA, Ward RJ. Accuracy and precision of joint space width measurements in standard and macroradiographs of osteoarthritic knees. Ann Rheum Dis. 1995 Nov; 54(11):872–80. [PubMed: 7492235]
4. Neumann G, Hunter DJ, Nevitt MC, Chibnik L, Kwoh K, Chen H, et al. Location specific radiographic joint space width for osteoarthritis progression. Osteoarthritis Cartilage. 2009 Jun; 17(6):761–5. [PubMed: 19073368]
5. Sharma L, Song J, Felson DT, Cahue S, Shamiyeh E, Dunlop DD. The role of knee alignment in disease progression and functional decline in knee osteoarthritis. JAMA. 2001 Jul 11; 286(2):188–95. [PubMed: 11448282]

6. Cerejo R, Dunlop DD, Cahue S, Channin D, Song J, Sharma L. The influence of alignment on risk of knee osteoarthritis progression according to baseline stage of disease. Arthritis Rheum. 2002 Oct; 46(10):2632–6. [PubMed: 12384921]
7. Muir P, McCarthy J, Radtke CL, Markel MD, Santschi EM, Scollay MC, et al. Role of endochondral ossification of articular cartilage and functional adaptation of the subchondral plate in the development of fatigue microcracking of joints. Bone. 2006 Mar; 38(3):342–9. [PubMed: 16275175]
8. Lane NE, Nevitt MC. Osteoarthritis, bone mass, and fractures: how are they related? Arthritis Rheum. 2002 Jan; 46(1):1–4. [PubMed: 11817580]
9. Burr DB. The importance of subchondral bone in osteoarthrosis. Curr Opin Rheumatol. 1998 May; 10(3):256–62. [PubMed: 9608330]
10. Goker B, Sumner DR, Hurwitz DE, Block JA. Bone mineral density varies as a function of the rate of joint space narrowing in the hip. J Rheumatol. 2000 Mar; 27(3):735–8. [PubMed: 10743818]
11. Westacott, CI. Subchondral bone in the pathogenesis of osteoarthritis. Biological effects. In: Brandt, KD.Doherty, M., Lohmander, LS., editors. Osteoarthritis. 2. Oxford: Oxford University Press; 2003. p. 133-42.
12. Radin EL, Abernethy PJ, Townsend PM, Rose RM. The role of bone changes in the degeneration of articular cartilage in osteoarthrosis. Acta Orthop Belg. 1978 Jan; 44(1):55–63. [PubMed: 665194]
13. Radin EL, Paul IL, Lowy M. A comparison of the dynamic force transmitting properties of subchondral bone and articular cartilage. J Bone Joint Surg Am. 1970 Apr; 52(3):444–56. [PubMed: 5425639]
14. Radin EL, Paul IL, Tolkoff MJ. Subchondral bone changes in patients with early degenerative joint disease. Arthritis Rheum. 1970 Jul; 13(4):400–5. [PubMed: 4246869]
15. Radin EL, Rose RM. Role of subchondral bone in the initiation and progression of cartilage damage. Clin Orthop Relat Res. 1986 Dec.213:34–40.
16. Eckstein F, Muller-Gerbl M, Putz R. Distribution of subchondral bone density and cartilage thickness in the human patella. J Anat. 1992 Jun; 180(Pt 3):425–33. [PubMed: 1487436]
17. Altman RD, Gold GE. Atlas of individual radiographic features in osteoarthritis, revised. Osteoarthritis Cartilage. 2007; 15(Suppl A):A1–A56. [PubMed: 17320422]
18. Brunet-Imbault B, Lemineur G, Chappard C, Harba R, Benhamou CL. A new anisotropy index on trabecular bone radiographic images using the fast Fourier transform. BMC Med Imaging. 2005 May 31.5:4. [PubMed: 15927072]
19. Jiang C, Pitt RE, Bertram JE, Aneshansley DJ. Fractal-based image texture analysis of trabecular bone architecture. Med Biol Eng Comput. 1999 Jul; 37(4):413–8. [PubMed: 10696694]
20. Pothuaud L, Lespessailles E, Harba R, Jennane R, Royant V, Eynard E, et al. Fractal analysis of trabecular bone texture on radiographs: discriminant value in postmenopausal osteoporosis. Osteoporos Int. 1998; 8(6):618–25. [PubMed: 10326070]
21. Benhamou, CL., Harba, R., Lespessailles, F., Jacquet, G., Tourliere, D., Jeanne, R. Changes in fractal dimension of trabecular bone in osteoporosis: a preliminary study. In: Nonnenmacher, TF.Losa, GA., Weibel, ER., editors. Fractals in Biology and Medicine. Basel, Switzerland: Birkhaüser Verlage; 1994. p. 292-9.
22. Yi WJ, Heo MS, Lee SS, Choi SC, Huh KH. Comparison of trabecular bone anisotropies based on fractal dimensions and mean intercept length determined by principal axes of inertia. Med Biol Eng Comput. 2007 Apr; 45(4):357–64. [PubMed: 17323084]
23. Pothuaud L, Benhamou CL, Porion P, Lespessailles E, Harba R, Levitz P. Fractal dimension of trabecular bone projection texture is related to three-dimensional microarchitecture. J Bone Miner Res. 2000 Apr; 15(4):691–9. [PubMed: 10780861]
24. Muller R. The Zurich experience: one decade of three-dimensional high-resolution computed tomography. Top Magn Reson Imaging. 2002 Oct; 13(5):307–22. [PubMed: 12464744]
25. Luo G, Kinney JH, Kaufman JJ, Haupt D, Chiabrera A, Siffert RS. Relationship between plain radiographic patterns and three-dimensional trabecular architecture in the human calcaneus. Osteoporos Int. 1999; 9(4):339–45. [PubMed: 10550451]

26. Turner CH, Rho JY, Ashman RB, Cowin SC. The dependence of elastic constants of cancellous bone upon structural density and fabric. Trans Orthop Res Soc. 1998; 13:74.
27. Peterfy C, Li J, Zaim S, Duryea J, Lynch J, Miaux Y, et al. Comparison of fixed-flexion positioning with fluoroscopic semi-flexed positioning for quantifying radiographic joint-space width in the knee: test–retest reproducibility. Skeletal Radiol. 2003 Mar; 32(3):128–32. [PubMed: 12605275]
28. Inglis D, Pietruszczak S. Characterization of anisotropy in porous media by means of linear intercept measurements. Int J Solids Struct. 2003; 40(5):1243–64.
29. Durand EP, Ruegsegger P. Cancellous bone structure: analysis of high-resolution CT images with the run-length method. J Comput Assist Tomogr. 1991 Jan; 15(1):133–9. [PubMed: 1987182]
30. Parfitt AM. Bone histomorphometry: standardization of nomenclature, symbols and units. Summary of proposed system. Bone Miner. 1988 Apr; 4(1):1–5. [PubMed: 3191270]
31. Wong AKO, Inglis D, Beattie KA, Doan A, Ioannidis G, Obeid J, et al. Reproducibility of computer-assisted joint alignment measurement in OA knee radiographs. Osteoarthritis Cartilage. 2009 May; 17(5):579–85. [PubMed: 19027328]
32. Kraus VB, Vail TP, Worrell T, McDaniel G. A comparative assessment of alignment angle of the knee by radiographic and physical examination methods. Arthritis Rheum. 2005 Jun; 52(6):1730–5. [PubMed: 15934069]
33. Moreland JR, Bassett LW, Hanker GJ. Radiographic analysis of the axial alignment of the lower extremity. J Bone Joint Surg Am. 1987 Jun; 69(5):745–9. [PubMed: 3597474]
34. Petersson IF, Boegard T, Svensson B, Heinegard D, Saxne T. Changes in cartilage and bone metabolism identified by serum markers in early osteoarthritis of the knee joint. Br J Rheumatol. 1998 Jan; 37(1):46–50. [PubMed: 9487250]
35. Buckland-Wright JC, Messent EA, Bingham CO III, Ward RJ, Tonkin C. A 2 yr longitudinal radiographic study examining the effect of a bisphosphonate (risedronate) upon subchondral bone loss in osteoarthritic knee patients. Rheumatology (Oxford). 2007 Feb; 46(2):257–64. [PubMed: 16837470]
36. Bennell KL, Creaby MW, Wrigley TV, Hunter DJ. Tibial subchondral trabecular volumetric bone density in medial knee joint osteoarthritis using peripheral quantitative computed tomography technology. Arthritis Rheum. 2008 Sep; 58(9):2776–85. [PubMed: 18759296]
37. Bruyere O, Dardenne C, Lejeune E, Zegels B, Pahaut A, Richy F, et al. Subchondral tibial bone mineral density predicts future joint space narrowing at the medial femoro-tibial compartment in patients with knee osteoarthritis. Bone. 2003 May; 32(5):541–5. [PubMed: 12753870]
38. Shimizu M, Tsuji H, Matsui H, Katoh Y, Sano A. Morphometric analysis of subchondral bone of the tibial condyle in osteoarthrosis. Clin Orthop Relat Res. 1993 Aug.293:229–39.
39. Dequeker J, Boonen S, Aerssens J, Westhovens R. Inverse relationship osteoarthritis–osteoporosis: what is the evidence? What are the consequences? Br J Rheumatol. 1996 Sep; 35(9):813–8. [PubMed: 8810662]
40. Buckland-Wright JC. Subchondral bone changes in hand and knee osteoarthritis detected by radiography. Osteoarthritis Cartilage. 2004; 12:S10–9. [PubMed: 14698636]
41. Karvonen RL, Miller PR, Nelson DA, Granda JL, Fernandez-Madrid F. Periarticular osteoporosis in osteoarthritis of the knee. J Rheumatol. 1998 Nov; 25(11):2187–94. [PubMed: 9818663]
42. Fazzalari NL, Parkinson IH. Femoral trabecular bone of osteoarthritic and normal subjects in an age and sex matched group. Osteoarthritis Cartilage. 1998 Nov; 6(6):377–82. [PubMed: 10343770]
43. Neuman P, Hulth A, Linden B, Johnell O, Dahlberg L. The role of osteophytic growth in hip osteoarthritis. Int Orthop. 2003; 27(5):262–6. [PubMed: 12844237]
44. Lane LB, Bullough PG. Age-related changes in the thickness of the calcified zone and the number of tidemarks in adult human articular cartilage. J Bone Joint Surg Br. 1980 Aug; 62(3):372–5. [PubMed: 7410471]
45. Stevens SS, Beaupre GS, Carter DR. Joint loading regulates the development of articular cartilage thickness. Trans Orthop Res Soc. 1998; 23:900.
46. Carter DR, Wong M. The role of mechanical loading histories in the development of diarthrodial joints. J Orthop Res. 1988; 6(6):804–16. [PubMed: 3171761]

47. Bettica P, Cline G, Hart DJ, Meyer J, Spector TD. Evidence for increased bone resorption in patients with progressive knee osteoarthritis: longitudinal results from the Chingford study. Arthritis Rheum. 2002 Dec; 46(12):3178–84. [PubMed: 12483721]

48. Brown AN, McKinley TO, Bay BK. Trabecular bone strain changes associated with subchondral bone defects of the tibial plateau. J Orthop Trauma. 2002 Oct; 16(9):638–43. [PubMed: 12368644]

49. Takahashi S, Tomihisa K, Saito T. Decrease of osteosclerosis in subchondral bone of medial compartmental osteoarthritic knee seven to nineteen years after high tibial valgus osteotomy. Bull Hosp Jt Dis. 2002; 61(1–2):58–62. [PubMed: 12828381]

50. Imhof H, Sulzbacher I, Grampp S, Czerny C, Youssefzadeh S, Kainberger F. Subchondral bone and cartilage disease: a rediscovered functional unit. Invest Radiol. 2000 Oct; 35(10):581–8. [PubMed: 11041152]

51. Li B, Aspden RM. Mechanical and material properties of the subchondral bone plate from the femoral head of patients with osteoarthritis or osteoporosis. Ann Rheum Dis. 1997 Apr; 56(4): 247–54. [PubMed: 9165997]

52. Bobinac D, Spanjol J, Zoricic S, Maric I. Changes in articular cartilage and subchondral bone histomorphometry in osteoarthritic knee joints in humans. Bone. 2003 Mar; 32(3):284–90. [PubMed: 12667556]

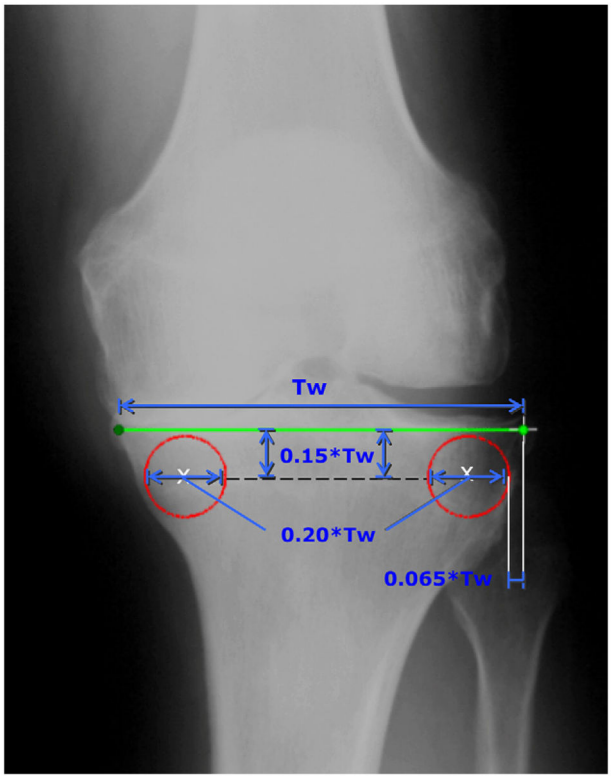

Fig. 1.

Placement of locater-rule endpoints on anatomic landmarks in knee radiograph for identification of subchondral ROIs. Endpoints of a locator rule (Tw) were positioned on the non-osteophytic tibial borders just inferior to the tibial plateau cortical plates (bone–cartilage interface). Constructed ROIs were placed at certain distances as a function of Tw, away from landmarks.

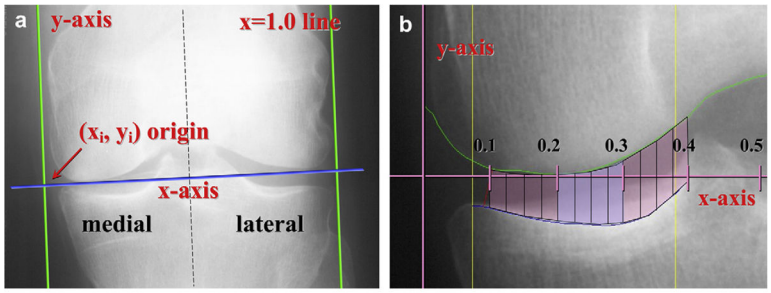

Fig. 2.

(a) Placement of coordinate axes for JSW(*x*) measurement in knee radiographs: *x*-axis tangential to femoral epicondyles; *y*-axis and *x* = 1.0 line positioned at the femoral contour edge, perpendicular to the *x*-axis; (b) Defining specific sites along *x*-axis where JSW(*x*) was determined.

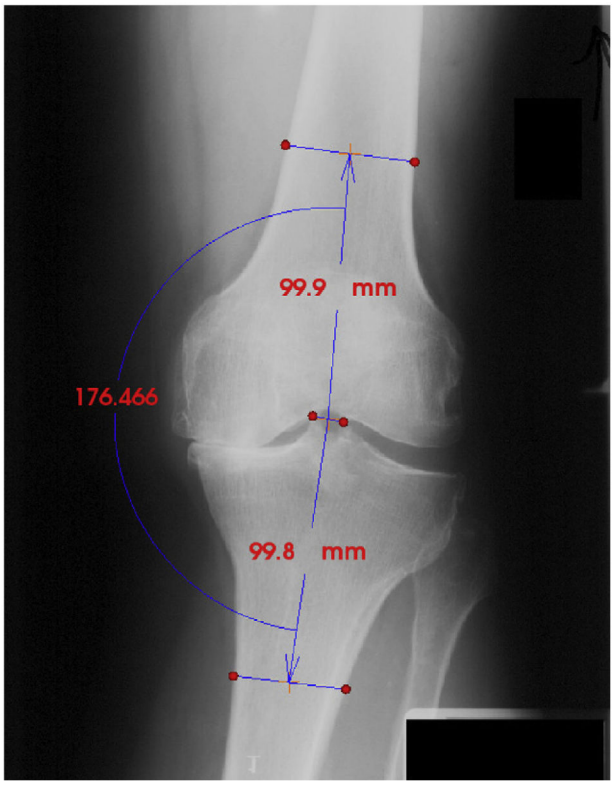

Fig. 3.

KA angle assessment using a custom algorithm and a defined set of anatomic landmarks. The centre rule in the middle was placed on the tibial spine tips. Both femoral and tibial rules were positioned within 10.0 ± 0.5 cm from the centre rule with endpoints placed on outer cortical shell and aligned parallel to the tibial plateau. Anatomic angle (θ_A) was separately converted to a mechanical angle (θ_M) according to an equation determined by Kraus and colleagues[32]: $\theta_M = (0.69 \times \theta_A) + 53.69$.

Table I

Mathematical and logical definitions of apparent topological and run-length BTX parameters where L = sum of all run-lengths; ΣI = sum of all bone run-lengths; $L - \Sigma I$ = sum of all soft-tissue run-lengths; N_b = number of bone run-lengths; N_t = number of tissue run-lengths; SL = skeletal length; N_{SL} = number of continuous skeletal lengths; δ = isotropic pixel spacing[28]

Apparent BTX parameter/calculated from (B = binary images, S = skeletonized images)		Logical definition	Mathematical definition
BVTV	BVTV (B)	Proportion of bone run-lengths to total run-lengths	$\frac{\sum I}{L} \times 100\,(\%)$
Tb.Sp	Tb.Sp (B)	Average of all soft-tissue run-lengths	$\frac{2 \times (L - \sum I) \times \delta}{\pi \times N_t}(\mathrm{mm})$
Tb.Th	Tb.Th (B)	Average of all trabecular bone run-lengths	$\frac{2 \times \sum I \times \delta}{\pi \times N_b}(\mathrm{mm})$
FE	Number of free trabecular ends (S)	Count of trabecular terminal ends (units)	[Count]
NL	NL (S)	Measure of average trabecular length	$(\Sigma SL)/N_{SL} \times \delta$ (mm)
Nd	Number of nodes (S)	Count of intersection points between trabeculae (units)	[Count]
CI	CI (S)	Index measure of connectedness of trabeculae	$\frac{Nd - FE}{NL} \times 100\,(\%)$

Table II

Characteristics of participants in the pre-arthroplasty population with advanced-stage knee OA including anthropometrics and disease characteristics

Participant characteristic	Mean and error where appropriate
Sex	17 women, 13 men
Age (years)	66 ± 9
BMI (kg m^{-2})	31.1 ± 6.0
WOMAC global score	41.6 ± 16.1
KL score (number distribution)	1 Grade 1, 5 Grade 2, 5 Grade 3, 27 Grade 4
Number of affected knees (number with bilateral OA)	38 (with eight pairs) (19 left, 19 right)
Number of medial compartment lesions	26
Number of lateral compartment lesions	12
Number of dual compartment lesions	4

Table III

Reproducibility of subchondral BTX parameter measurements from semi-automated software algorithm as reported by RMSCV% and root-mean square SD (RMSSD)

Subchondral BTX parameters	RMSCV%	RMSSD
BVTV (%)	1.07	0.0031
Tb.Th (μm)	0.94	2.2
Tb.Sp (μm)	1.06	5.7
FE (count)	6.29	4.59
NL (mm)	5.74	3.33
Nd (count)	9.87	1.80
CI (%)	11.11	0.62

Table IV

BTX parameters obtained in the subchondral region of the proximal tibia in the affected compartment in plain knee radiographs of severe OA participants requiring TKA expressed as means (±2 SD)

	Mean (±2SD)
BVTV (%)	33.01 (25.41, 40.61)
CI (%)	−6.684 (−12.448, −0.920)
FE (count cm^{-2})	29.26 (22.59, 28.93)
NL (mm)	27.88 (18.76, 37.01)
Nd (count cm^{-2})	8.68 (3.18, 14.18)
Tb.Th (μm)	229.3 (187.6, 271.0)
Tb.Sp (μm)	436.3 (329.7, 542.9)

Table V

Simultaneous multivariate linear regression analysis, reporting correlation coefficients between Tb.Sp and JSW(x) at locations (a) $x = 0.200$, (b) $x = 0.225$, (c) $x = 0.250$ and (d) $x = 0.275$ in knee OA participants with medial compartment disease ($N = 26$) [B units: Tb.Sp μm mm^{-2}/mm JSW(x)]

Covariate adjustment	*B*	*P*-Value	Lower CI	Upper CI	*B*	*P*-Value	Lower CI	Upper CI
	(a) Tb.Sp vs JSW(x = 0.200)				*(b) Tb.Sp vs JSW(x = 0.225)*			
Unadjusted	0.036	0.446	−0.059	0.131	0.035	0.432	1.576	2.063
Gender	0.055	0.077	−0.006	0.117	0.049	0.098	−0.010	0.109
Gender and BMI	**0.068**	**0.044**	**0.002**	**0.134**	0.060	0.062	−0.003	0.124
	(c) Tb.Sp vs JSW(x = 0.250)				*(d) Tb.Sp vs JSW(x = 0.275)*			
Unadjusted	0.033	0.420	−0.049	0.115	0.032	0.367	−0.039	0.102
Gender	0.044	0.105	−0.010	0.098	0.037	0.115	−0.040	0.084
Gender and BMI	0.056	0.060	−0.003	0.114	0.048	0.064	−0.003	0.099

Bold: indicates statistical significance at the $\alpha = 0.05$ level.

Table VI

Simultaneous multivariate linear regression analysis, reporting correlation coefficients between the area-adjusted number of FE and JSW(x) at locations (a) $x = 0.200$, (b) $x = 0.225$, (c) $x = 0.250$ and (d) $x = 0.275$ in knee OA participants with medial compartment disease ($N = 26$) [B units: FE units × 10^{-3} mm^{-2}/mm JSW(x)]

Covariate adjustment	*B*	*P*-Value	Lower CI	Upper CI	*B*	*P*-Value	Lower CI	Upper CI
	(a) Area-adjusted FE vs JSW(x = 0.200)				*(b) Area-adjusted FE vs JSW(x = 0.225)*			
Unadjusted	−3.86	0.372	−12.6	4.892	−3.92	0.340	−12.24	4.40
BMI	−7.59	0.062	−15.585	0.399	−7.42	0.054	−14.98	0.15
mKAD and BMI	−8.93	0.077	−18.924	1.059	−8.86	0.066	−18.35	0.63
	(c) Area-adjusted FE vs JSW(x = 0.250)				*(d) Area-adjusted FE vs JSW(x = 0.275)*			
Unadjusted	−3.43	0.358	−10.986	4.129	−2.78	0.389	−9.33	3.76
BMI	**−7.17**	**0.043**	**−14.075**	**−0.259**	**−6.29**	**0.041**	**−12.32**	**−0.27**
mKAD and BMI	**−8.99**	**0.047**	**−17.834**	**−0.151**	**−7.94**	**0.044**	**−15.66**	**−0.21**

Bold: indicates statistical significance at the $\alpha = 0.05$ level.

Table VII

Simultaneous multivariate linear regression analysis of area-adjusted (a) trabecular FE, (b) Tb.Sp and (c) number of nodes (Nd) with mJSW in TKA participant digitized knee radiographs (N = 34) as measured by a semi-automated software algorithm [B units: number of FE × 10^{-3} mm^{-2}/mm JSW(x); Tb.Sp μm mm^{-2}/mm JSW(x); number of Nd × 10^{-3} mm^{-2}/mm JSW(x)]

Covariate adjustment	*B*	*P*-value	Lower CI	Upper CI
(A) Area-adjusted FE vs mJSW				
Unadjusted	−6.97	0.092	−15.78	1.21
BMI	**−10.97**	**0.006**	−18.53	**−3.40**
BMI and rKAD	**−12.25**	**0.004**	**−20.16**	**−4.34**
(B) Tb.Sp vs mJSW				
Unadjusted	0.064	0.196	−0.035	0.162
Gender	**0.077**	**0.017**	**0.015**	**0.139**
Gender and BMI	**0.098**	**0.004**	**0.034**	**0.161**
(C) Area-adjusted Nd vs mJSW				
Unadjusted	−5.41	0.115	−12.21	1.40
Age	**−7.40**	**0.039**	**−14.39**	**−0.41**
Age and rKAD	**−10.08**	**0.005**	**−16.85**	**−3.31**

Bold: significance at the α = 0.05 level.